

In-situ localized carbon nanotube growth inside partially sealed enclosures

Y. van de Burgt, A. Champion, and Y. Bellouard

Citation: *AIP Advances* **3**, 092119 (2013); doi: 10.1063/1.4821952

View online: <http://dx.doi.org/10.1063/1.4821952>

View Table of Contents: <http://scitation.aip.org/content/aip/journal/adva/3/9?ver=pdfcov>

Published by the [AIP Publishing](#)



Goodfellow

metals • ceramics • polymers
composites • compounds • glasses

Save 5% • Buy online
70,000 products • Fast shipping

***In-situ* localized carbon nanotube growth inside partially sealed enclosures**

Y. van de Burgt,^{1,2,a} A. Champion,¹ and Y. Bellouard¹

¹*Department of Mechanical Engineering, Eindhoven University Technology, Den Dolech 2, Eindhoven, The Netherlands.*

²*Holst Centre/TNO – Netherlands Organization for Applied Scientific Research, HTC31, Eindhoven, The Netherlands.*

(Received 12 July 2013; accepted 6 September 2013; published online 18 September 2013)

Carbon nanotube assemblies can be used for specific applications such as sensors and filters. We present a method and proof-of-concept to directly grow vertically-aligned carbon nanotube structures within sealed enclosures by means of a feedback-controlled laser-assisted chemical vapor deposition technique. The process is compatible with a variety of micro-fabrication processes and bypasses the need for post-process packaging. Our experiments raise interesting observations related to the gas diffusion dynamics in micro-scale and sub-micron enclosures. © 2013 Author(s). All article content, except where otherwise noted, is licensed under a Creative Commons Attribution 3.0 Unported License. [<http://dx.doi.org/10.1063/1.4821952>]

I. INTRODUCTION

Owing to their special geometrical, structural and electrical properties, carbon nanotubes (CNTs) have been found to be useful in applications such as sensors¹ and filters^{2,3} among many others. Their organic nature also allows them to be used in micro-fluidic biological applications and makes them compatible with many materials commonly used in micro-fluidics, such as PDMS or glass. For instance, vertically aligned carbon nanotube embedded structures have been proposed for enhanced particle interception in cell separation^{4,5} and as blood pressure sensors.⁶

These applications use lithography in combination with thermal chemical vapor deposition (CVD) to control the geometry of the nanotube structure and embed the nanotubes inside the device by creating the micro-channel on top of the nanotubes. More convenient would be to directly grow the nanotubes inside the micro-channel without the need of an extra structuring or transfer step. Various techniques for local growth of carbon nanotube structures such as micro-resistive heating⁷ or micro-induction⁸ have been proposed. Although these techniques provide the possibility of localized heating and CNTs growth, it has intrinsically limited flexibility.

In this paper, we present a laser-assisted fabrication method for local *in-situ* growth of carbon nanotube structures inside enclosures. This technique eliminates the lithography structuring step and increases the versatility of the process since a laser-beam can be used virtually anywhere in the channel. Specifically, as a proof-of-principle, we show the growth of a hill of vertically aligned carbon nanotubes inside a micro-channel created by femtosecond laser processing. Furthermore, we also demonstrate the growth of CNTs on a silicon substrate covered with a transparent window. This result raises interesting questions related to gas diffusion kinetics.

II. EXPERIMENTAL

Carbon nanotube chemical vapor deposition (CVD) growth consists of a thermal energy supply, a catalyst and a carbon-containing precursor gas. This growth method provides a high degree of control making it the most promising method for carbon nanotube growth.

^aAuthor to whom correspondence should be addressed. Electronic mail: y.b.v.d.burgt@tue.nl



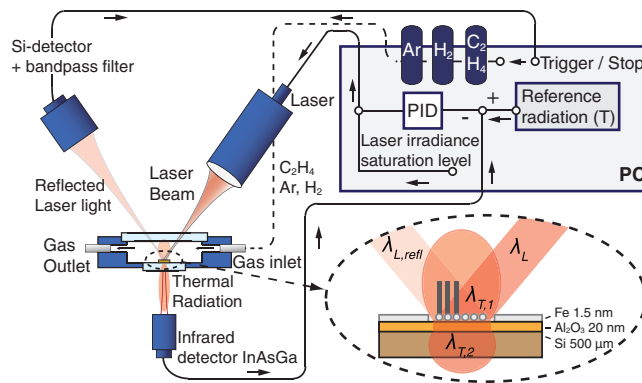


FIG. 1. Schematic overview of the closed-loop control laser-assisted growth of carbon nanotubes. The arrows depict the flow of operation. The thermal radiation from the substrate is controlled by means of a feedback signal from the infrared detector. The reflected laser light is collected by a Si-detector with a bandpass-filter to isolate the laser wavelength. The gas flow is laminar over the substrate and can be individually controlled. The inset illustrates the formation of the nanoparticles (right) on the catalyst followed by the CNT growth (left) on the substrate during laser irradiation.

Among CVD processes, laser-assisted ones differ from conventional CVD by using a laser to provide the thermal energy. This opens up new possibilities for direct-write growth as well as fast and local heating, enabling the growth site to be surrounded by temperature-sensitive elements and/or materials. Indeed, the laser-assisted CVD growth method is compatible with most polymers and other materials or adhesives used in micro-fluidics. Inherent to the use of local heating is the non-uniform temperature distribution. Laser heating can also induce some possible overheating due to the dynamically varying absorptivity of the substrate during the CNTs growth process.⁹ To bypass these issues, we use a temperature closed-loop controlled laser-assisted CVD process using emitted thermal radiation from the laser spot as feedback (a schematic of this setup is presented in Fig. 1). Further control of the process is achieved by monitoring a photodetector signal measuring the variation of intensity of the reflected laser light from the growth site. This closed-loop control process is described in more detail elsewhere.¹⁰

In this experiment, the micro-channel is fabricated in a 500 μm-thick fused-silica glass slide with lateral dimensions similar to the substrate, 4 × 4 mm on which it stands. A femtosecond laser process was combined with etching for 24 hours in 2.5% hydrogen-fluoride (HF) solution to create the channel.¹¹ The open channel is 1 mm wide, 120 μm in height and has a length of 4 mm. For aligned carbon nanotube growth we use a silicon substrate covered with a 20 nm Al₂O₃ and a 1.5 nm iron catalyst layer both deposited by electron-beam evaporation. The laser used is a continuous-wave (CW) diode laser operating at a wavelength of 808 nm, focused to a spot of about 500 μm. To visualize and analyze the resulting CNT structures grown inside the channel by scanning electron microscopy (SEM), the channel was not permanently attached to the substrate. However, to show the proof-of-concept, Epotek 355nd epoxy is used to glue the two parts together at the side-edges of the substrate, so that the material combination can withstand the elevated temperatures around the laser hot spot. Other bonding processes such as anodic bonding could also be considered and are assumed to be more stable for the high temperatures involved here.

In Fig. 2(a) a schematic of the channel growth is presented. The laser beam is focused onto the substrate through the fused silica channel, which is transparent to the wavelength of the laser, 808 nm. The channel itself only has two openings where the gas flows through.

III. RESULTS AND DISCUSSION

The proof-of-concept is presented in Fig. 3(a) with a photo of the locally grown CNT structure inside the attached micro-channel. In Fig. 3(b) a photo of the transparent micro-channel attached to the substrate is shown with the inset showing the (infrared) light emission from inside the channel during growth.

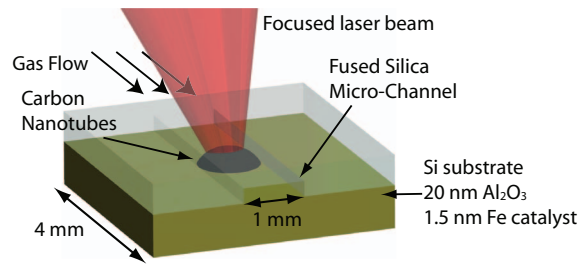


FIG. 2. Schematic of the direct local growth of carbon nanotubes inside a sealed micro-channel. For the second experiment, the same setup is used but without channel and just a window covering the substrate.

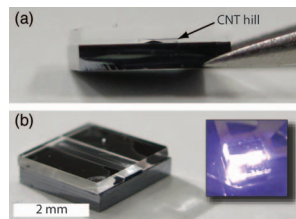


FIG. 3. A. Photo of the hill of aligned CNTs grown inside a sealed fused silica micro-channel attached to a silicon substrate. B. View of the channel. Inset shows a photo of the channel during laser-assisted growth.

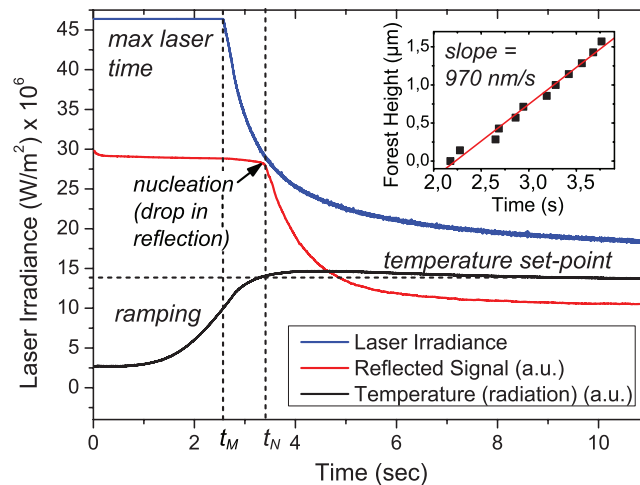


FIG. 4. Typical graphs plotting laser power and sensor signals as a function of time for *in situ* localized closed-loop controlled growth inside a micro-channel. The laser power is at a maximum level while ramping to the radiation set-point and drops (t_M) when this level is reached to keep the radiation constant. The reflection shows a clear drop indicating the nucleation of nanotube growth (t_N). Inset shows calculated forest height and corresponding growth rate.

The nucleation of nanotube growth is typically indicated by a drop in the reflected laser signal. This can be seen in Fig. 4 which shows a characteristic graph relating laser irradiance and sensor signals. The laser irradiance starts at the maximum level while ramping to the temperature set-point. Just before reaching this set-point, the reflected laser signal shows a clear drop, indicating the nucleation of the nanotube growth. The temperature reached at the laser spot is estimated using a finite element simulation¹⁰ and is about 900°C. The lateral distribution is of Gaussian nature and reaches about 420°C at the edges (i.e. at a distance of 2 mm). The heat can be significantly confined using a less conductive substrate than silicon, such as fused silica with a thermal conductivity of about 100 times lower.

From the reflected laser irradiance signal in Fig. 4 we also extracted forest height by measuring an interference effect of the reflected laser signal with the nanotube forest. This is shown in the inset

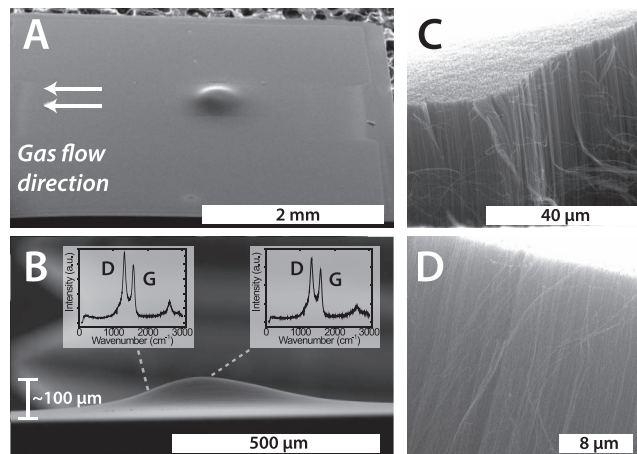


FIG. 5. Scanning Electron Micrographs of nanotube growth inside a micro-channel. A. Overview of the substrate with the hill of aligned nanotubes visible. Also depicted is the gas flow direction. B. Side view of the hill. Indicated is the estimated height. Inset shows a Raman intensity plot for this experiment. The ratio of D and G-band intensities indicate multiwall carbon nanotubes. C. Detailed zoom of the alignment of the nanotubes after scratching the hill. D. Detailed zoom of the other side after scratching.

of the figure. The calculated growth rate is $0.97 \mu\text{m/s}$ which corresponds to estimates made from scanning electron micrographs.

In Fig. 5 corresponding scanning electron micrographs of the resulting growth are presented. This particular nanotube structure was grown in 150 sec and has an estimated height of about $100 \mu\text{m}$. The lateral dimensions of the structure are about $800 \times 600 \mu\text{m}$. An overview of the substrate with corresponding CNT growth is shown in Fig. 5(a). In Fig. 5(b) a view of the side of the hill is given, from which the height was estimated. The insets show the Raman intensity signals for two positions on the sample. The ratio of D- and G-band intensities of the Raman signal can be used to evaluate the quality of the CNTs. Here, both signals indicate multi-walled CNTs, predicting the presence of a vertically aligned forest of multi-wall carbon nanotubes. In Fig. 5(c) and Fig. 5(d) detailed zooms of the aligned nanotubes are given. These pictures were obtained after scratching the nanotubes grown layer from the side in the direction of the gas flow. Fig. 5(c) shows a zoom of the left side of the hill while the Fig. 5(d) shows an enhanced zoom of the right side of the hill, visible by the slopes of the top of the nanotubes in both pictures.

Using a heat/flow coupled finite element simulation of the laser heated micro-channel we could investigate the effects of laser heating on the laminar flow (see Fig. 6). The laminar flow is essential for carbon nanotube growth as it ensures a stable and known gas feed to the laser heated spot. From the simulation we learned that the sudden increase in temperature by laser heating increases the Reynolds number significantly but still within laminar flow conditions. The flow quickly stabilizes again.

During these experiments we also observed “side-growth” of CNTs. It appears that when the fused-silica channel is not permanently attached to the substrate, nanotubes can grow in between the silicon substrate and the fused silica cover. Assuming both the silicon and the fused silica have a surface roughness in the nanometers range, it seems unlikely that the nanotubes can grow to lengths of $10 - 20 \mu\text{m}$ with only the carbon already present in between the two surfaces.

To investigate the phenomena, a series of test-experiments were performed on a substrate simply covered by a unattached fused silica window and using different process times, ranging from 25 seconds to 150 seconds with different gas flow ratios.

From these experiments it appeared that the further from the side, thus the closer to the laser irradiated center, the longer the nanotubes were. Two other direct relations between nanotube lengths were found with time and carbonaceous gas concentration. From these results we conclude that the process showed conventional growth behavior, where it appeared that it did not matter there was a fused silica cover covering the substrate and catalyst. In other words, the carbonaceous gas found

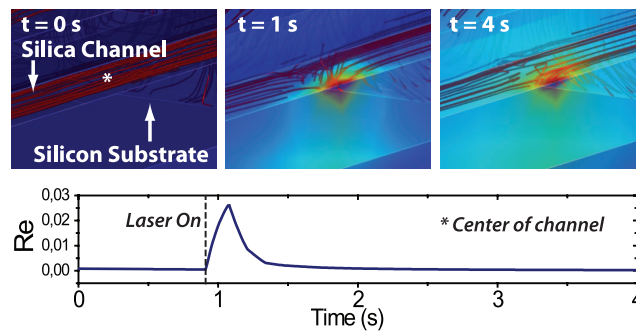


FIG. 6. Simulation of flow alteration by switching on the laser and corresponding Reynolds number measured in the center of the channel, just above the laser heated zone. At $t = 0$ s, the laminar flow is clearly visible and at $t = 1$ s, the streamlines are disrupted by the sudden increase in temperature as a result of the laser heating. At $t = 4$ s, the flow is stabilized again. The corresponding Reynolds number confirms this trend.

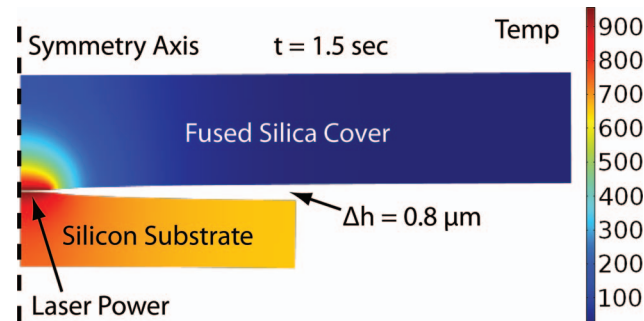


FIG. 7. Finite Element Method simulation in COMSOL linking the expansion to temperature for a given input laser irradiance. The figure shows the scaled result after 1.5 seconds. A gap of $0.8 \mu\text{m}$ has been created with the substrate reaching 900°C .

its way to the laser-induced hot spot rather easy. Much easier as one would expect by estimating diffusion lengths for the nano-channels in between the two surfaces.

A possible explanation is the very fast heating of both surfaces by the laser irradiance. From Fig. 4 we can see that for certain conditions the laser can operate at its maximum irradiance level for about 3 seconds. During this time the substrate and covering fused silica locally heat up quickly resulting in a temperature gradient which can result in thermally-induced bending. The bending of both surfaces could result in a large enough opening to allow the carbonaceous gas to flow to the nucleation site.

In Fig. 7 the results of a Finite Element Method simulation of material expansion with COMSOL Multiphysics are presented. A radial symmetric model of the substrate is simulated with heating by a constant laser irradiance corresponding to the maximum laser power in Fig. 4. The resulting temperature variation over time is used as the input on a similar model of the fused silica glass. The two pictures are assembled for clarification. The time after which the resulting gap is calculated is chosen to be 1.5 seconds for two reasons. First of all, the gap does not increase much more after this time, due to heat conduction through the material. Secondly, after 1.5 seconds the temperature in the model starts to deviate from reality due to the simplified thermal conditions in the model. The resulting gap of $0.8 \mu\text{m}$ might be enough for the carbonaceous gas to enter and flow to the laser hot spot nucleation site. Due to the consumption of the ethylene gas and precipitation into carbon nanotubes in the center, a pressure difference is created between the center of the laser-heated zone and the outside. An estimation of the diffusion length of ethylene yields about 9 mm for these particular conditions. However, the walls of the sub-micro enclosure are expected to reduce this length significantly. Despite the temperature gradient in the channel, the diffusion in combination with the pressure driven flow, seem like a plausible explanation for the growth. However, further analysis is desirable.

IV. CONCLUSION

We have presented a laser-assisted closed-loop controlled carbon nanotube growth process that has the capability of growing locally aligned carbon nanotube structures inside a sealed micro-channel. As a result of the local heating the process is compatible with a variety of packaging technologies that may use adhesive, polymers or other temperature sensitive material.

The use of a laser makes the process versatile, enabling the growth of nanotubes at arbitrary positions within enclosure such as a micro-channel as demonstrated here. In addition, laser-assisted growth also opens up possibilities of scanning the laser within a cavity giving the possibility to create arbitrary patterns in an enclosure. For instance, this could be useful for lab-on-a-chip applications for creating filters.³

To add even more flexibility to the process by removing the requirement of a deposited nanolayer, the catalyst could also be part of the gas feed, for instance using iron pentacarbonyl gas, Fe(CO)₅. In addition, to get absorption within a fluidic channel made of a transparent material, a non-linear absorption process such as multi-photons could be used. For instance, using femtosecond laser exposure of silica in the cumulative regime produces localized heat affected zones.¹²

Furthermore, we observed the growth of CNTs on a simple substrate fully covered with a fused silica glass window. The growth took place in a relatively short time (from 25 s to 150 s). This observation raises interesting questions concerning diffusion of gases inside sub-microns channels.

ACKNOWLEDGMENTS

The authors wish to thank A. Frijns and S.V. Gaastra - Nedeia for helpful suggestions.

¹ J. Kong, N. R. Franklin, C. Zhou, M. G. Chapline, S. Peng, K. Cho, and H. Dai, *Science* **287**, 622 (2000).

² A. Srivastava, O. N. Srivastava, S. Talapatra, R. Vajtai, and P. M. Ajayan, *Nat. Mater.* **3**, 610 (2004).

³ T. Guan and M. Yao, *J. Aerosol Sci.* **41**, 611 (2010).

⁴ G. D. Chen, F. Fachin, M. Fernandez-Suarez, B. L. Wardle, and M. Toner, *Small* **7**, 1061 (2011).

⁵ G. D. Chen, F. Fachin, E. Colombini, B. L. Wardle, and M. Toner, *Lab. Chip* **12**, 3159 (2012).

⁶ A. T. Sepúlveda, F. Fachin, R. G. de Villoria, B. L. Wardle, J. C. Viana, A. J. Pontes, and L. A. Rocha, *Procedia Eng.* **25**, 140 (2011).

⁷ O. Englander, D. Christensen, and L. Lin, *Appl. Phys. Lett.* **82**, 4797 (2003).

⁸ B. D. Sosnowchik and L. Lin, *Appl. Phys. Lett.* **89**, 193112 (2006).

⁹ M. Haluska, Y. Bellouard, Y. van de Burgt, and A. Dietzel, *Nanotechnology* **21**, 7 (2010).

¹⁰ Y. van de Burgt, Y. Bellouard, R. Mandamparambil, M. Haluska, and A. Dietzel, *J. Appl. Phys.* **112**, 034904 (2012).

¹¹ Y. Bellouard, A. Said, M. Dugan, and P. Bado, *Opt. Express* **12**, 2120 (2004).

¹² C. B. Schaffer, J. F. García, and E. Mazur, *Appl. Phys.* **76**, 351 (2003).